

# MODELLING OF TEMPERATURE FIELDS AND STRESS-STRAIN STATE OF SMALL 3D SAMPLE IN ITS LAYER-BY-LAYER FORMING\*

O.V. MAKHNENKO<sup>1</sup>, A.S. MILENIN<sup>1</sup>, E.A. VELIKOIVANENKO<sup>1</sup>, N.I. PIVTORAK<sup>1</sup> and D.V. KOVALCHUK<sup>2</sup>

<sup>1</sup>E.O. Paton Electric Welding Institute, NASU

11 Kazimir Malevich Str., 03680, Kiev, Ukraine. E-mail: office@paton.kiev.ua

<sup>2</sup>PJSC SPE «Chervona Khvylya»

15 Kazimir Malevich Str., 03680, Kiev, Ukraine. E-mail: master@chervonahvilya.com

A set of investigations on kinetics of temperature fields and stress-strain state of a tee section was carried out employing mathematical and computer modelling methods in order to optimize a process of layer-by-layer forming of titanium structural elements of aerospace designation by means of current xBeam 3D Metal Printer (xBeam) electron beam technologies. The results of investigations were used for temperature fields optimizing in order to provide uniform distribution on height and length of the product by selection of efficient time between deposition passes of forming beads and source alternating power. Besides, typical stress and strain fields, formed in the product during its manufacture, were shown as well as possibilities of application of processing methods for reduction of residual forming. 26 Ref., 2 Tables, 13 Figures.

**Keywords:** *layer-by-layer forming, electron beam, temperature field, stress-strain state, optimizing, mathematical modelling*

Currently, the additive technologies are an alternative to traditional manufacture of titanium structural elements with complex geometry, first of all in aerospace industry and medicine [1–9]. It is caused by the fact that cost of remelting of titanium alloy scrap, being a result of machining of medium- and large-size parts, is higher in the majority of cases than the expenses for layer-by-layer forming of such type of objects. In the case with small-size parts this increases productivity of manufacture of the one-of-a kind samples by individual order.

There are several different approaches to production of metallic structures based on principle of layer-by-layer object forming. These approaches differ on types of consumables and used heat sources. They can be divided on two main groups by types of used consumables, namely sintering or fusion of metallic powders [1, 2, 5–10] and deposition with consumable (filler wires etc.) feeding [1, 4, 11–13].

The methods using flux-cored consumables allow producing complex geometry objects with high accuracy of performance, in particular, for manufacture of 3D porous structures [1–3, 5–8, 10, 14–17]. Such types of structures are successfully used in medicine as implants [7, 9, 13, 18]. At that, deposition rate is

extremely low that limits application of these technologies for medium- and large-size structures.

A rate of deposition using technology based on filler wires is significantly higher in the majority of cases by order. Besides, in such approaches efficiency of consumables application is also significantly higher and can reach 100 % [1].

The heat sources in approaches using filler wires are laser, electron beam or electric arc. The approaches based on laser technologies are the most popular in current time due to their accuracy [1, 4, 12, 19], nevertheless their energy efficiency is low (2–5 %) [1–4]. Electron beam deposition differs by great efficiency, but requires high vacuum. The results of metal structure examinations show that electron beam deposition allows producing complex-shape parts with homogeneous structure of metal in the deposited layers similar to base metal (substrate) structure [20]. This is a reason why this procedure is the most perspective in aerospace industry [3, 4].

The main disadvantage of the methods using metallic wire deposition is appearance of significant residual stresses and deformations [13]. High residual stresses can significantly reduce service characteristics of produced components, particularly, their dura-

\*Based on a report presented at the VIII International Conference «Mathematical Modelling and Information Technologies in Welding and Related Processes», September 19–23, 2016, Odessa, Ukraine.

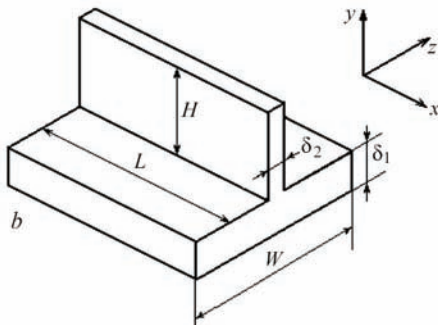
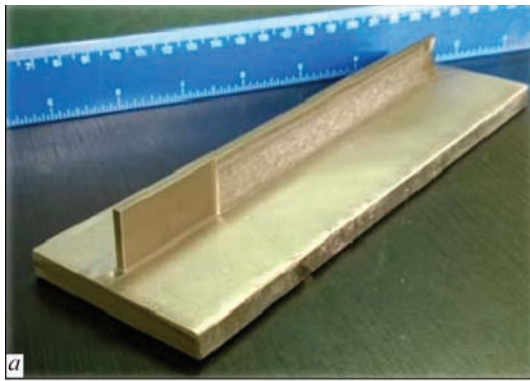


**Figure 1.** Appearance (a) and scheme (b) of tee section of titanium alloy, produced by electron beam multilayer forming

bility at cyclic loads, and residual deformations can result in unallowable distortion of shape and rejection of part billets.

Optimizing the additive deposition technologies applying mathematical modelling for decrease of volume of experimental investigations requires substantial computer and time expenses [11, 15]. However, selection of the optimum deposition parameters based on computer prediction is the most promising.

**Manufacturing scheme of process of multilayer forming of 3D samples.** Figure 2 shows xBeam manufacturing scheme by example of multilayer forming of tee section (Figure 1). The process takes place under conditions of medium vacuum (in the range of  $10^{-2}$  mbar), that, on the one hand, allows eliminating metal contamination due to high affinity with oxy-

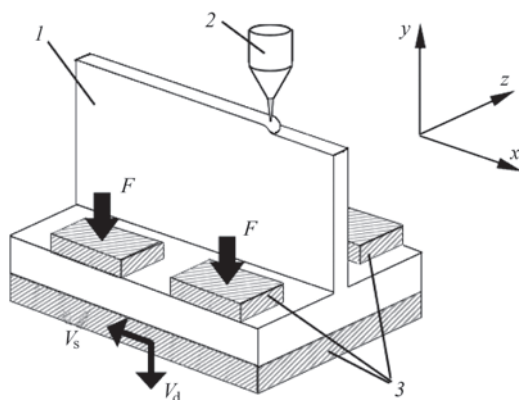


**Figure 2.** Process scheme of electron beam multilayer forming of tee section samples: 1 — part being formed; 2 — modulus of heating and wire feed; 3 — process fixture

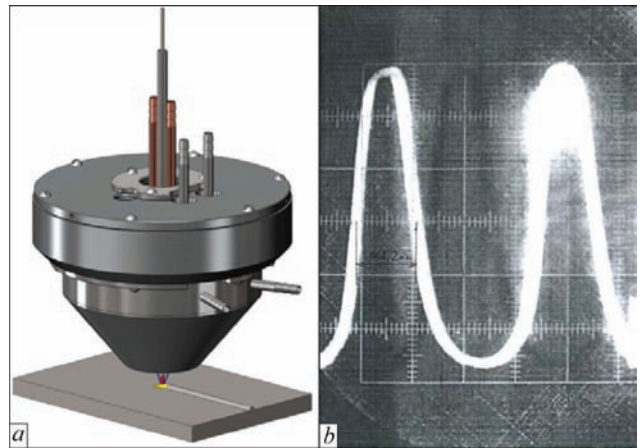


**Figure 3.** Scheme of electron beam heating (a) modulus and experimentally determined distribution of energy flow in electron beam (b)

gen and/or nitrogen, and on the other hand, provides sufficient focusing of electron beam. Substrate of the product being formed (in considered case it is tee section flange) is located in a pre-stressing fixture, which presses it to movable platform with force  $F$ , and moves it relatively stationary heat source with set rate  $V_s$  in a plate plane and periodically, with deposition of each bead, in normal direction with rate  $V_d$ .

The heat source is a joined complex of systems for generation of electron beam in form of hollow cone, having maximum close convergence on a surface of structure being formed, and filler wire feed (Figure 3, a). This allows performing efficient and sufficiently uniform melting of filler wire without its significant overheating as well as forming melt pool on the substrate or earlier deposited layer for quick spread of liquid filler material over the surface. Figure 3, b shows experimentally determined distribution of energy flow in such electron beam.

In accordance with laboratory investigations, the product as a result of layer-by-layer deposition got specific residual bending deformation as a consequence of formation of welding shrinkage of metal in the deposition area. Besides, the preliminary experiments showed that the end areas are characterized by irregular structure of section wall as a result of non-uniform heating in deposition. One of the advantages of used xBeam scheme is the possibility of program control of heat input that provides wide possibilities for optimizing the parameters of the considered process. Variation of a delay time between deposition of each bead and reasonable selection of method and level of preheating are also efficient optimizing parameters.

**Investigation procedure.** Software package WeldPrediction, developed at the E.O. Paton Electric Welding Institute of the NAS of Ukraine for prediction of physical-mechanical processes in welding and related technologies [21–23], was used for prelim-

inary analysis of state kinetics in the sample of tee section of titanium alloy. Solution of the problems of heat conductivity and stress-strain state of metal in preheating, further deposition up to part cooling and removal of process fixture was carried out on joint rectangular partitioning meshes. Shape of the product was changed at each deposition stage in accordance with deposition rate and geometry of beads forming at that. It is reasonable to solve nonstationary thermoplasticity problem in 2D definition by averaging 3D calculation temperature field on thickness. This allows examining development of state of investigated product with sufficient accuracy, and reducing investigation resource intensity.

Thus, finite-difference solution of 3D nonstationary equation of heat conductivity was used for numerical analysis of kinetics of temperature field  $T(x, y, z)$  on time  $t$  in xBeam deposition of the part, shown in Figure 1:

$$c\gamma(T)\frac{\partial T}{\partial t} = \nabla[\lambda(T)\nabla T], \quad (1)$$

where  $c\gamma$ ,  $\lambda$  are the specific heat capacity and heat conductivity of material, respectively.

The boundary conditions, necessary for problem solution (1), depend on heat sink from the product surface. Thus, heat sink in the area of contact with process fixture can be described by Newton's law, while on a free surface it is characterized by heat radiation (Stefan–Boltzmann law) with additional energy input from product end being deposited in the case of heat source location in that place. Thus, boundary conditions for solution of heat conductivity problem in the studied case have the following form:

$$-\lambda(T)\frac{\partial T}{\partial n} = \begin{cases} \alpha_T(T - T_C), & \text{in the area of contact with fixture} \\ \varepsilon\sigma_{SF}(T^4 - T_C^4) - q, & \text{on free surfaces,} \end{cases} \quad (2)$$

where  $n$  is the normal to surface;  $\alpha_H$  is the heat sink coefficient;  $T_E$  is the environment temperature;  $\varepsilon$  is the material emissivity factor;  $\sigma_{SF}$  is the Stefan–Boltzmann constant;  $q$  is the energy flow of electron beam heating.

A relationship between components of stress and strain tensors can be stated by generalized Hooke's law considering temperature volumetric changes and associated law of plastic flow [24, 25]:

$$\begin{cases} \Delta\varepsilon_{ij} = \psi(\sigma_{ij} - \delta_{ij}\sigma_m) + \delta_{ij}(K\sigma_m + \Delta\varepsilon_T) - b_{ij} \\ b_{ij} = \frac{1}{2G}(\sigma_{ij} - \delta_{ij}\sigma_m)^* + (K\sigma_m)^* \end{cases} \quad (3)$$

$(i, j) = (x, y, z),$

where  $K = (1 - 2\nu)/E$ ;  $E$  is the Young's modulus;  $\nu$  is the Poisson's ratio;  $G = E/(2(1 + \nu))$ ;  $\Delta\varepsilon_T$  is the deformation increment, caused by metal thermal expansion;

$\psi$  is the function of material state, determined by yield condition, namely:

$$\psi = \begin{cases} \frac{1}{2G}, & \text{if } \sigma_i < \sigma_T(T), \\ \frac{1}{2G}, & \text{if } \sigma_i = \sigma_T(T), \end{cases} \quad (4)$$

where

$$\sigma_i = \frac{1}{\sqrt{2}} \sqrt{(\sigma_{xx} - \sigma_{yy})^2 + (\sigma_{xx} - \sigma_{zz})^2 + (\sigma_{yy} - \sigma_{zz})^2 + 6(\sigma_{xy}^2 + \sigma_{xz}^2 + \sigma_{yz}^2)}$$

Plastic strains are determined from equation

$$\Delta\varepsilon_{ij} = \left(\psi - \frac{1}{2G}\right)(\sigma_{ij} - \delta_{ij}\sigma_m), \quad (i, j = x, y, z). \quad (5)$$

Realization of condition (4) is carried out at each step of tracing,  $\sigma_{ij}$  stresses are presented from (5) at that each  $\psi$  iteration in form of

$$\begin{cases} \sigma_{ij} = \frac{1}{\psi} \left( \Delta\varepsilon_{ij} + \delta_{ij} \frac{\psi - K}{K} \Delta\varepsilon \right) + J_{ij}; \\ J_{ij} = \frac{(b_{ij} - \delta_{ij}b) + \delta_{ij} \left( K\sigma^* - \frac{\Delta\varepsilon_T}{K} \right)}{\psi}, \end{cases} \quad (6)$$

where

$$\Delta\varepsilon = \frac{\Delta\varepsilon_{xx} + \Delta\varepsilon_{yy} + \Delta\varepsilon_{zz}}{3}, \quad b = \frac{b_{xx} + b_{yy} + b_{zz}}{3}.$$

Relationship between  $\Delta\varepsilon_{ij}$  tensor and vector of displacement increment  $\Delta U_i$  is presented in the following way

$$\Delta\varepsilon_{ij} = \frac{\Delta U_{i,j} + \Delta U_{j,i}}{2}, \quad (7)$$

where coma corresponds to differentiation.

A resolving system of algebraic equations in relation to displacement increment vector in the nodes of finite elements at each step of tracing and  $\psi$  iteration is determined as a result of its functional minimizing (Lagrange variation principle)

$$E_l = -\frac{1}{2} \sum_V (\sigma_{ij} + J_{ij}) \Delta\varepsilon_{ij} V_{m,n,r} + \sum_{S_p} P_i \Delta U_i \Delta S_P^{m,n,r}, \quad (8)$$

where  $\sum_V, \sum_{S_p}$  are the operators of sum on internal and superficial finite elements, respectively;  $P_i$  is the power vector of external influence ( $i = x, y, z$ ).

Thus, a set of equations, which allows solution in regard to the vector of displacement increments at each step of tracing and  $\psi$  iteration for corresponding finite element, looks like:

$$\begin{cases} \frac{\partial \Delta U_l}{\partial \Delta U_{m,n,r}} = 0; \\ \frac{\partial \Delta U_l}{\partial \Delta V_{m,n,r}} = 0; \\ \frac{\partial \Delta U_l}{\partial \Delta W_{m,n,r}} = 0. \end{cases} \quad (9)$$

**Table 1.** Process parameters of multilayer forming of laboratory titanium alloy sample (working gas — helium)

| Parameter  | Value                | Notes  |
|--|----------------------|--|
| Consumable (rod)   | Diameter 1.6 mm      | Titanium of VT1-0 grade                          |
| Substrate (plate)  | 8×30×70 mm           | Titanium of VT1-0 grade                          |
| Vacuum   | $5 \cdot 10^{-1}$ Pa | Vacuum reduced to 1 Pa after start of gas supply |
| Accelerating voltage   | 15 kV                | —  |
| Electron beam current  | 300 mA               | —  |
| Electron beam power  | 4.5 kW               | —  |
| Consumable feed rate   | 14 mm/s              | —  |
| Rate of substrate movement on axis <i>X</i>                    | 14 mm/s              | —  |
| Displacement on axis <i>Y</i> before each new deposition cycle | 0.5 mm               | —  |
| Number of deposited layers                                     | 37                   | —  |

Solution of indicated problems of nonstationary thermal plasticity according to given mathematical description was carried out by means of numerical tracing of elasto-plastic deformations, starting from a stage of substrate preheating, deposition of each bead up to complete cooling of the product and removal of process fixture, in scope of respective finite element description [26].

**Modelling results.** Considered manufacturing process was modeled based on the results of laboratory investigations on deposition of titanium alloy tee product (Figure 1). Table 1 shows the main parameters of given manufacturing cycle.

Solution of the temperature problem shows (Figure 4) that the temperature fields of studied case have 3D nature, at that temperature in the deposited thin wall of tee section is distributed sufficiently uniform

along a cross-section and flange state is characterized by relatively low temperature gradients.

One of the main problems, which was studied at this stage of investigations, lied in study of potential possibilities for achievement of stationary temperature field in the product at each layer deposition. This allows acquiring favorable conditions of bead formation as well as providing uniformity of structural state of metal in all section of the product, and, respectively, homogeneity of its physical-mechanical and service properties. The results of numerical modelling according to procedure mentioned above show absence in bead deposition of significant overheating of liquid metal after coming on the surface of product being formed. This indicates effective heat sink in the metal of product and environment. This allows receiving sufficient heating-through for providing fu-

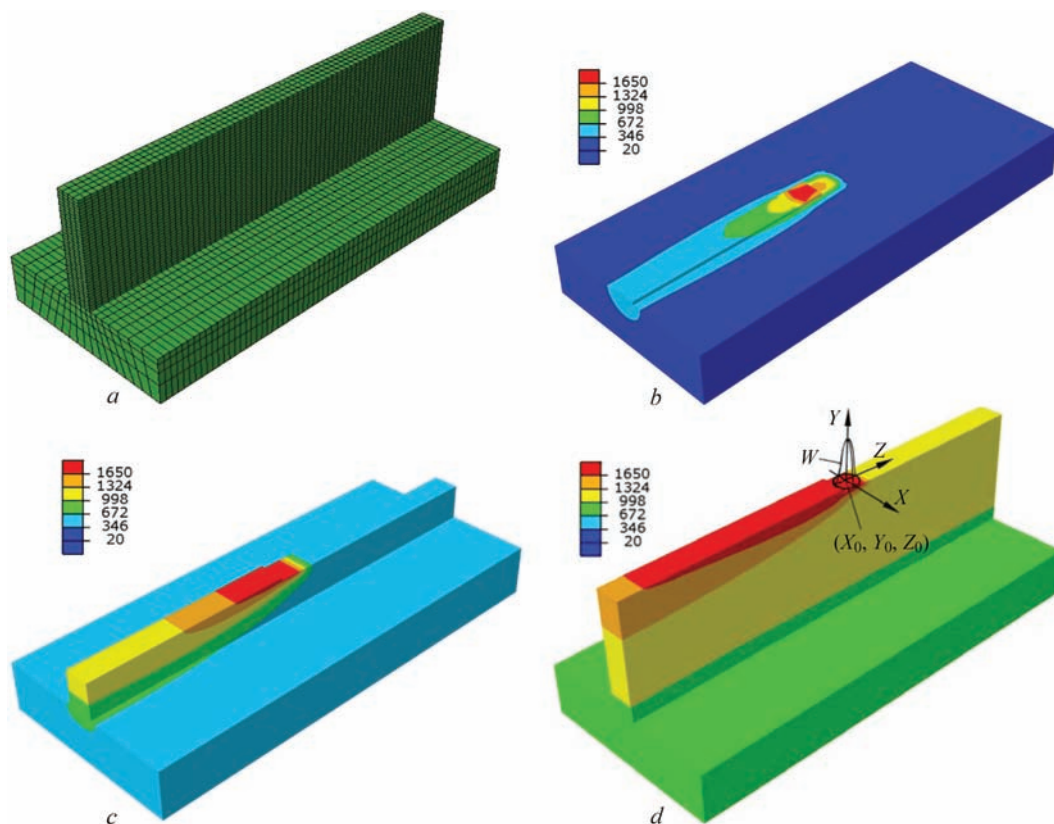


**Figure 4.** Finite-element model (*a*) and distribution of temperatures in tee sample during layer-by-layer forming: *b* — deposition of the 1<sup>st</sup> bead; *c* — deposition of the 12<sup>th</sup> bead; *d* — deposition of the 37<sup>th</sup> bead and scheme of model of distributed heat source

**Table 2.** Model modes of bead deposition in process of tee section product forming at alternating power of electron beam heat source

| Number of mode | Power of source in different areas of element being deposited, kW (%) |           |           |
|----------------|---|-----------|-----------|
|                | 0–2 mm  | 2–68 mm   | 68–70 mm  |
| 1              | 4.5 (100)   | 4.5 (100) | 4.5 (100) |
| 2              | 6.3 (140)   | 4.5 (100) | 4.3 (95)  |
| 3              | 7.2 (160)   | 4.5 (100) | 4.3 (95)  |

sion of beads and preventing overheating and excessive yield of liquid metal.

Typical peculiarity of distribution of the maximum temperatures at deposition area is locally lower temperatures in the beginning of bead and small overheating at the end. This can be balanced, in particular, by alternating power of electron beam heat source on length. Three modes of bead deposition (Table 2) were studied for example, namely basic one (1) and modes of excessive power at the beginning of deposition (2) and reduced at the end (3).

Selected modes use variation of source power at relatively small sections of deposited metal for balancing excessive heat sink in cold part at the beginning of melting and excessive heat accumulation close to end part of the edge, and reaching more uniform distribution of the maximum temperatures (Figure 5 as an example shows calculation distribution of temperatures in deposition of the tenth bead). Further rise of power at the initial stage of formation of tee section wall (more than 160 %) is not reasonable, since it will cause local overheating of given area of the structure.

In addition to provide the homogeneity of metal structural state in bead deposition direction it is also important to keep a temperature mode with the maximum approximation to stationary one in deposition of each wall layer of considered section for metal homogeneity on height. The results of calculations (Figure 6) show that the stationary mode takes place after

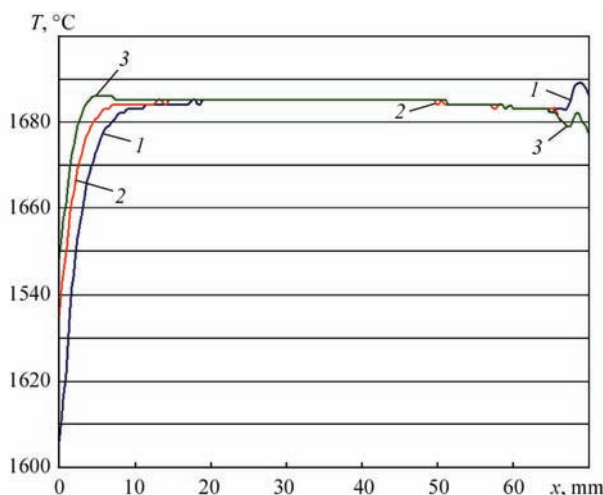


**Figure 5.** Distribution of maximum temperatures along the whole length of deposited bead for different modes of heat source effect (modes 1–3 according to Table 2)

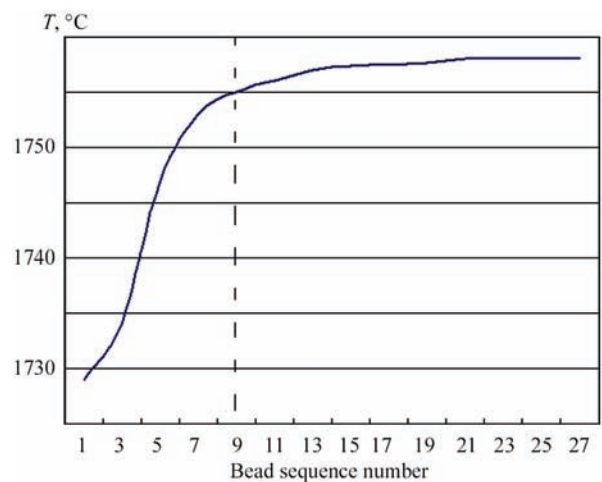


**Figure 6.** Dependence of space-averaged on bead section maximum temperature of deposited metal in the section central area on bead sequence number

the eighth bead. Temperature averaged on bead area in  $2.7 \cdot 10^{-3}$  s after its deposition in the central part of tee section was used as example.

One more important factor, which should to be considered in selection of reasonable parameters for deposition of investigated sample, is the delay time  $t_r$  between deposition of each bead. On the one hand, increase of the delay time allows more uniform redistribution of heat from each of deposit beads, on the other hand, decrease of  $t_r$  results in reduction of power intensity of studied process and less accumulation of heat energy by section. Figure 7 shows effect of  $t_r$  value on value of steady-state temperature in the product central area. It can be concluded from indicated data that overheating of deposited product edge up to remelting of previous deposited layer is observed at  $t_r < 25$  s. At  $t_r > 40$  s stationary mode is more preferable from point of view of quality of element being formed, but at that initial stage of deposition can be characterized by lack of fusion in the metal layers as

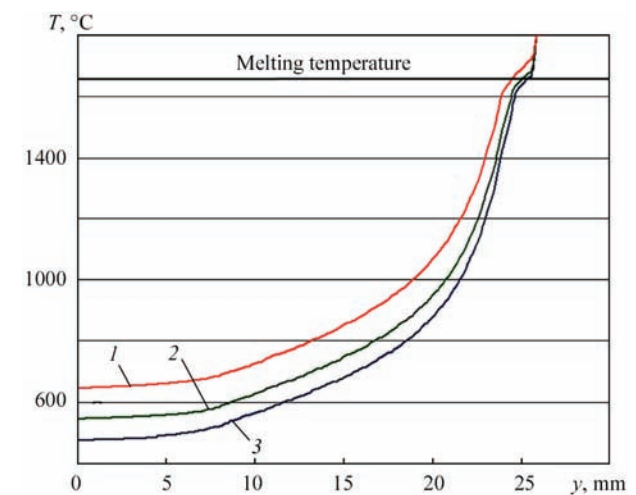


**Figure 7.** Distribution of maximum temperatures on section height in deposition of the 37<sup>th</sup> bead for different delay time between beads: 1 —  $t_r = 20$  s; 2 — 30; 3 — 40

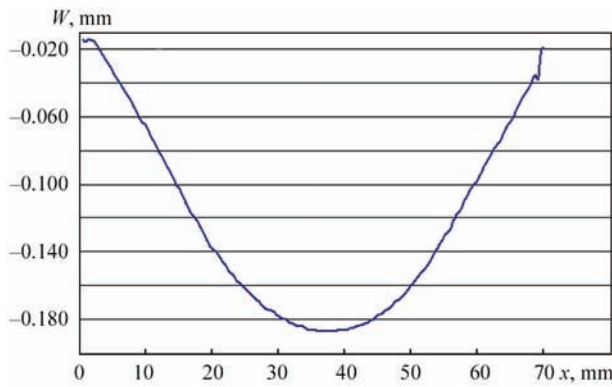


**Figure 8.** Residual forming of lower plane of product substrate of tee section after EBD ending, complete cooling and removal of pre-stressing fixture

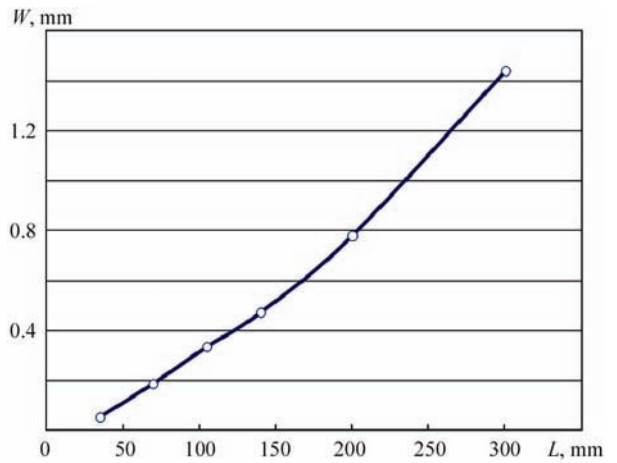


**Figure 9.** Dependence of residual bending deflection of tee section  $W$  on its length  $L$  after fixture removal

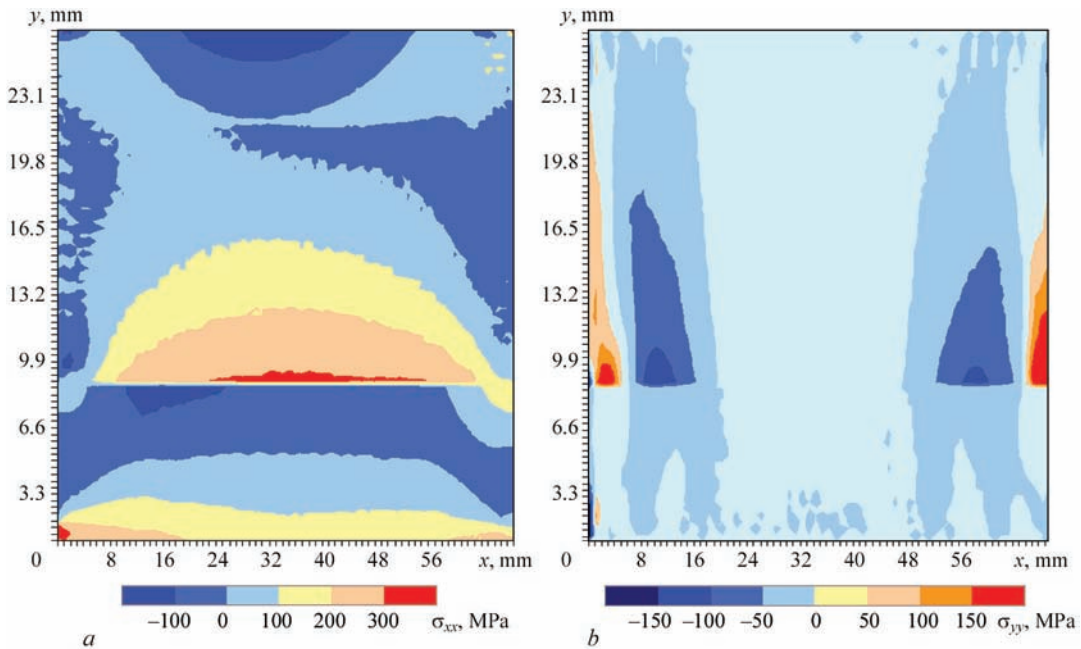


**Figure 10.** Distribution of residual stresses  $\sigma_{xx}$  and  $\sigma_{yy}$  in product after its forming at mode 1 (see Table 2)

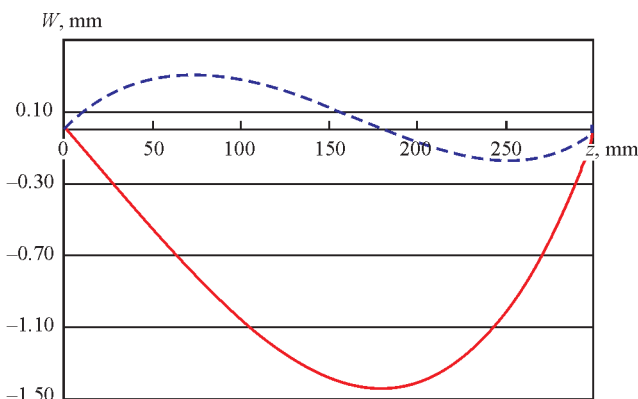


**Figure 11.** Shape of longitudinal axis of tee deposited sample  $L = 300$  mm after layer-by-layer forming on initially even substrate (solid line) and considering preliminary bending deflection  $W_0 = 1.5$  mm (dashed line)

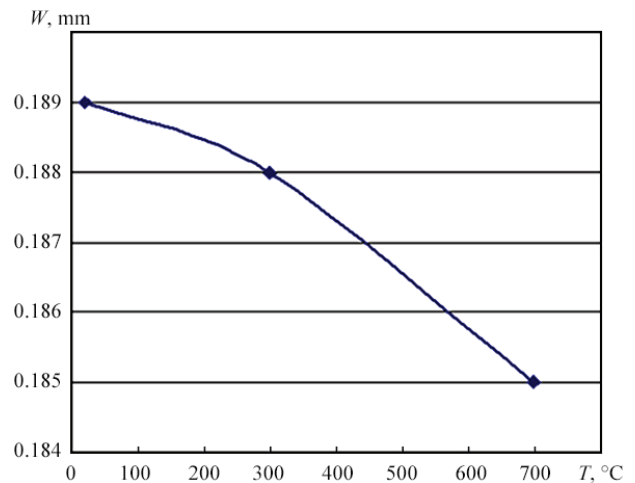


**Figure 12.** Dependence of residual bending deflection  $W$  of deposited sample  $L = 70$  mm after fixture removal on preheating temperature  $T_0$

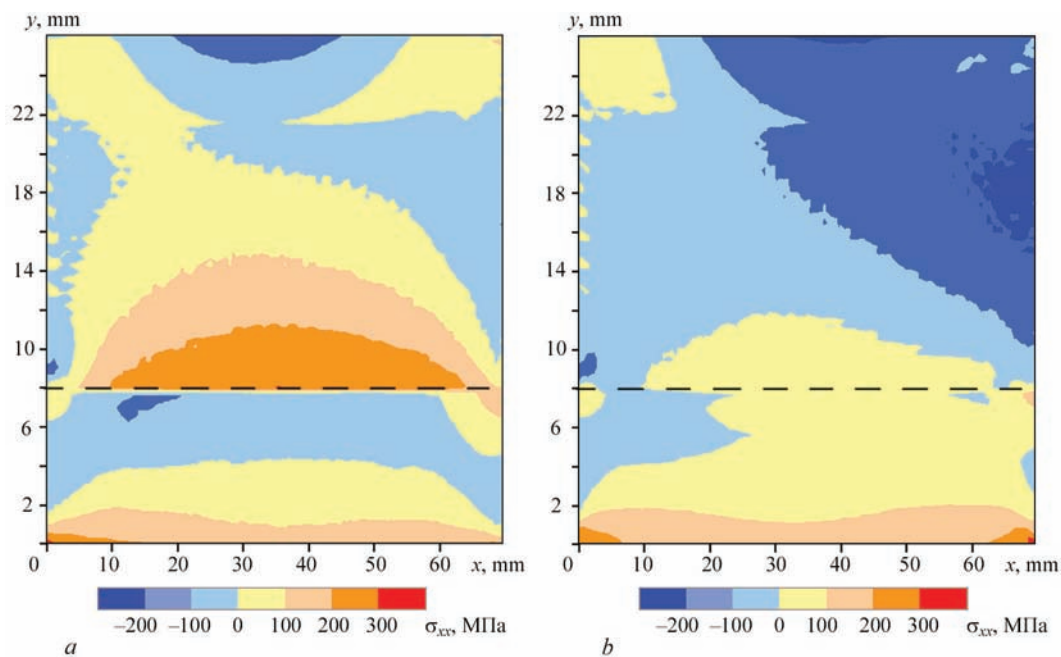


**Figure 13.** Distribution of longitudinal residual stresses  $\sigma_{xx}$  in product after its forming at substrate preheating to  $T_0 = 300$  (a) and  $700$  °C (b)

a result of intensive heat sink in the structure. Therefore,  $25 \text{ s} < t_r < 35 \text{ s}$  range can be considered as reasonable in selection of a regular delay of deposit of each bead in all height of the element being deposited.

Residual forming and internal stresses in the formed product can be the factors limiting application of considered technology. Irreversible deformations of the substrate of investigated element of tee section as a result of longitudinal shrinkage can exceed the allowances, prescribed by specific design solutions, while high residual stresses depress resistance to fatigue action and increase susceptibility to stress-corrosion fracture. Thermomechanical treatment is mostly used for improvement of service characteristics of the structures, in particular, welded ones. However, additional operating stage of product processing involves increase of prime cost, therefore optimizing the xBeam process taking into account the peculiarities of kinetics of stress-strain state of specific design structure is reasonable. Thus, residual strain on mechanism of longitudinal shrinkage is the most cenfavorable and typical for investigated product of tee section. As a result whole structure bends in longitudinal plane (Figure 8). Due to relatively small length of this element, its residual forming is insignificant (around  $0.2 \text{ mm}$ ), but residual deflection can go beyond the limits of necessary allowances (Figure 9) if rise of structure length is required.

Stressed state in the product plane (Figure 10) is characterized by relatively low level of residual stresses in longitudinal as well as transverse direction. Distinctive feature is some concentration of stresses  $\sigma_{yy}$  as a result of end effects. Besides, area of transition of the tee flange to the wall includes excessive longitudinal stresses  $\sigma_{xx}$ , caused by general structure bend.

An effective processing method for decrease of residual stresses in welded structures is preliminary bending deflection (flexure), which can be realized due to pre-stressing fixture. Figure 11 presents the results of calculation of bending deflection of an axis of tee deposited sample of  $L = 300 \text{ mm}$  length after layer-by-layer forming on initially even substrate and taking into account preliminary bending deflection  $W_0$ . It can be seen that the optimum value of preliminary bending deflection can significantly reduce residual deformations of general forming.

The results of evaluation of substrate preheating effect on residual deformations of tee sample of  $70 \text{ mm}$  length are given in Figure 12. The value of residual bending deflection in substrate heating from room temperature to  $700$  °C virtually does not change ( $2 \%$ ), and residual stresses in area of flange to wall transition significantly drop at heating temperature increase (Figure 13).

## Conclusions

1. A set of mathematical models and software means for their realizing was developed for numerical prediction of kinetics of temperature and stress-strain state of tee section structure of titanium alloy in process of electron-beam deposition by xBeam 3D Metal Printing. Typical peculiarities of temperature field distribution were investigated in terms of basic parameters of manufacture of laboratory samples of tee section. It is shown that specific stabilizing of the temperature cycles on length of deposited wall can be achieved by setting of alternating power of heat source, i.e. up to  $160 \%$  of power at initial stage for larger heating of product edge and less than  $95 \%$  of power at final

stage for balancing of heat accumulation process at the sample end.

2. Substantial effect of the delay duration between deposit of each of forming beads on nature of temperature distribution was shown, namely reduction of delay duration time less than 20 s results in significant accumulation of heat in the product metal and, as a result, significant overheating and excessive penetration, that can decrease quality of product being formed.

3. Formation of residual longitudinal bending deformations at 0.2 mm level is shown by means of numerical prediction of development of strained state of the product in the process of deposition, further cooling and relieve of fixture forces. At that variation of product length has significant effect on longitudinal bend value, that can require corresponding thermomechanical straightening. An effective processing method for reduction of residual deformations is preliminary bending deflection (flexure), which can be realized due to pre-stressing fixture.

4. Analysis of the results of prediction of residual stressed state of the examined model structure showed formation of excessive tensile longitudinal stresses in the area of tee section flange to wall transition that is caused by total structure bend. Besides, expressed stress concentrators  $\sigma_{yy}$  are formed in area of its ends. The results of evaluation of effect of preliminary substrate heating on stress-strain state of the tee sample showed that residual stresses in the flange to wall transition area essentially drops at rise of heating temperature and high tempering conditions are virtually provided at  $T_0 = 700$  °C.

*The authors express gratitude to G.F. Rozyńska and D.S. Gavrilov for participation in paper preparation.*

1. Ding, D. et al. (2015) Wire-feed additive manufacturing of metal components: Technologies, developments and future interests. *Int. J. of Adv. Manufact. Technology*, 81(1), 465–481.
2. Heintl, P. et al. (2007) Cellular titanium by selective electron beam melting. *Adv. Eng. Mater.*, 9, 360–364.
3. Kristofer, Ek. (2014) *Additive manufactured material*: Master of Sci. Thesis, Stockholm.
4. Brandl, E. et al. (2010) Additive manufactured Ti–6Al–4V using welding wire: Comparison of laser and arc beam deposition and evaluation with respect to aerospace material specifications. *Physics Procedia*, December, 595–606.
5. Mandil, G. et al. (2016) Building new entities from existing titanium part by electron beam melting: Microstructures and mechanical properties. *Int. J. of Adv. Manufact. Technology*, Vol. 85, Issue 5, 1835–1846.
6. Murr, L.E. et al. (2010) Characterization of titanium aluminum alloy components fabricated by additive manufacturing using electron beam melting. *Acta Materialia*, Vol. 58, Issue 5, 1887–1894.
7. Marin, E. et al. (2010) Characterization of cellular solids in Ti6Al4V for orthopaedic implant applications: Trabecular

- titanium. *Mechan. Behaviour of Biomedical Mater.*, Vol. 3, Issue 5, 373–381.
8. Wahyudin P. Syam et al. (2012) Preliminary fabrication of thin-wall structure of Ti6Al4V for dental restoration by electron beam melting. *Rapid Prototyping J.*, April, 230–240.
9. Leonard F. et al. (2012) Assessment by X-ray CT of the effects of geometry and build direction on defects in titanium ALM parts. In: *Proc. of Conf. on Industrial Computed Tomography (ICT)*, 85–93.
10. Golkovski, M.G. et al. (2013) Atmospheric electron-beam surface alloying of titanium with tantalum. *Mater. Sci. & Engineering, A*, Vol. 578, 310–317.
11. Yan Ma et al. (2015) Effect of interpass temperature on in-situ alloying and additive manufacturing of titanium aluminides using gas tungsten arc welding. *Adv. Manufacturing*, 8, 71–77.
12. Blanka A. Szost et al. (2015) A comparative study of additive manufacturing techniques: Residual stress and microstructural analysis of CLAD and WAAM printed Ti–6Al–4V components. *Materials and Design*, Vol. 89, 559–567.
13. Baurfeld, B. et al. (2010) Additive manufacturing of Ti-6Al-4V components by shaped metal deposition: Microstructure and mechanical properties. *Materials and Design*, Vol. 31, 106–111.
14. Edwards, P. et al. (2013) Electron beam additive manufacturing of titanium components: Properties and performance. *J. of Manufact. Sci. and Engineering*, Vol. 135, Issue 6, 061016/1–061016/7.
15. Gong, X. et al. (2013) Powder-bed electron-beam-melting additive manufacturing: Powder characterization, process simulation and metrology. *ASME Early Career Techn. J.*, 12, 59–66.
16. Nai, M.L.S. et al. (2016) Recent progress of additive manufactured Ti-6Al-4V by electron beam melting. In: *Proc. of 27<sup>th</sup> Annual Int. Solid Freeform Fabrication Symp. — An Additive Manufacturing Conf.*, 691–704.
17. Petrovic, V. et al. (2012) Additive manufacturing solutions for improved medical implants. *Biomedicine, InTechOpen*, March, 147–180.
18. Jia, Lv et al. (2015) Electron beam melting fabrication of porous Ti6Al4V scaffolds: Cytocompatibility and osteogenesis. *Adv. Eng. Mater.*, 1–8.
19. Mari Koike et al. (2011) Evaluation of titanium alloys fabricated using rapid prototyping technologies — electron beam melting and laser beam melting. *Materials*, 4, 1776–1792.
20. Akhonin, S.V., Vrzhezhevsky, E.L., Belous, V.Yu. et al. (2016) Electron beam 3D-deposition of titanium parts. *The Paton Welding J.*, 5/6, 130–133.
21. Makhnenko, V.I. (2013) Problems of examination of modern critical welded structures. *Ibid.*, 5, 21–28.
22. Makhnenko, V.I., Velikoivanenko, E.A., Olejnik, O.I. (2008) Risk analysis as a method for formalizing decision making on unscheduled repair of welded structures. *Ibid.*, 5, 2–7.
23. Milenin, O.S. (2011) Probabilistic analysis of state of main pipelines with revealed defects and their service life after repair under pressure. *Visnyk Ternopil NTU*, Special Issue, Pt 1, 73–81.
24. Makhnenko, V.I. (1976) *Computational methods of investigation of welding stress and strain kinetics*. Kiev: Naukova Dumka.
25. Makhnenko, V.I. (2006) *Safety service life of welded joints and assemblies of modern structures*. Ibid.
26. Velikoivanenko, E.A. et al. (2014) Methods and technologies of parallel calculations for mathematical modeling of stress-strain state of structures taking into account ductile fracture. *Probl. Upravleniya i Informatiki*, 6, 42–52.

Received 14.02.2017